
Article:
de Melo Quintela, B., Hervas-Raluy, S., Garcia-Aznar, J.M. et al. (2022) A theoretical analysis of the scale separation in a model to predict solid tumour growth. Journal of Theoretical Biology, 547. 111173. ISSN: 0022-5193

https://doi.org/10.1016/j.jtbi.2022.111173

A Theoretical Analysis of the Scale Separation in a Model to Predict Solid Tumour Growth

Bárbara de Melo Quintela; Silvia Hervas-Raluy; Jose Manuel Garcia Aznar; Dawn Walker; Kenneth Y Wertheim; Marco Viceconti

Abstract—Solid tumour growth depends on a host of factors which affect the cell life cycle and extracellular matrix vascularization that leads to a favourable environment. The whole solid tumour can either grow or wither in response to the action of the immune system and therapeutics. A personalised mathematical model of such behaviour must consider both the intra- and inter-cellular dynamics and the mechanics of the solid tumour and its microenvironment. However, such wide range of spatial and temporal scales can hardly be modelled in a single model, and require the so-called multiscale models, defined as orchestrations of single-scale component models, connected by relation models that transform the data for one scale to another. While multiscale models are becoming common, there is a well-established engineering approach to the definition of the scale separation, e.g., how the spatiotemporal continuum is split in the various component models. In most studies scale separation is defined as natural, linked to anatomical concepts such as organ, tissue, or cell; but these do not provide reliable definition of scales: for examples skeletal organs can be as large as 500 mm (femur), or as small as 3 mm (stapes). Here we apply a recently proposed scale-separation approach based on the actual experimental and computational limitations to a patient-specific model of the growth of neuroblastoma. The resulting multiscale model can be properly informed with the available experimental data and solved in a reasonable timeframe with the available computational resources.

Keywords — Multiscale Model, neuroblastoma, Tumour growth modelling

INTRODUCTION

Cancer's rising prominence as the second leading cause of death partly reflects the declining mortality rates of stroke and coronary heart disease, relative to cancer, in many countries. There were an estimated 19.3 million new cases and 10 million cancer deaths worldwide in 2020 [1]. Therefore, cancer has a significant impact in all human societies. It is a complex and heterogeneous disease due to the variety of biological and mechanical factors at

different scales: tumour, stroma, cellular, and subcellular/molecular. In solid tumours the stroma includes connective tissue and blood vessels [2]. The occurrence and development of cancer are highly regulated by the biomechanical properties and cellular composition of the tissue microenvironment [3]. Therefore, it is essential to understand the biomechanical cues that favour the development of a primary tumour from isolated or clustered cancer cells.

Solid tumours in vivo exist in three main stages: the avascular, vascular, and metastatic phases. In the initial phase, namely the avascular stage, the primary mass grows quite rapidly due to cellular replication and the production of extracellular matrix. Beyond a certain size, it starts to compress surrounding tissues and organs. This primary tumour mass can achieve a few millimetres in diameter and its growth is strongly dependent on the mechanical properties of the extracellular microenvironment [4][5]. As the tumour grows, the cells at its centre undergo cell death due to a lack of nutrients, forming a necrotic core. However, beyond a certain stage, the tumour can develop its own vasculature by a process of angiogenesis. During this vascular phase, new blood vessels supply the tumour with nutrients and thus, enable rapid tumour growth. During the metastatic phase, some cancer cells migrate from the primary tumour, penetrate blood vessels, and ultimately, colonise distant sites [6].

Cancer cells can give rise to the above phenomena as an emergent outcome of a number of cellular phenotypic changes, or hallmarks: sustained proliferative signalling and evasion of growth suppressors, resistance to cell death, secretion of molecules inducing angiogenesis, replicative immortality, and their metastatic potential [7]. For example, many cell cycle proteins such as D-type and E-type cyclins are overexpressed or overactive in cancer cells, leading to uncontrolled proliferation [8]. The p53 tumour suppressor that triggers apoptosis in transformed cells is frequently mutated and subverted in cancer cells [9]. Various telomere maintenance mechanisms are associated with aggressive cancer types (including high-risk neuroblastoma) [10]. High expression of angiogenic factors by the cells in the tumour microenvironment is also common [11].

If the tumour is left untreated, it grows with a rate dependent on the genetic makeup of the tumour cells, the cell-to-tissue volume ratio (cellularity), and the extent of vascularisation. When treated with chemotherapy or radiotherapy, both the replication rates and cell death

rates are altered by the treatment, to an extent that again, depends on the above factors and the actual pharmacokinetics (drug delivery in each part of tumour mass) [12]. Computational models simulating biological processes are widely used to better understand the underlying mechanisms of biological phenomena, including cancer progression [13]. There are diverse approaches to model tumour growth, including discrete methods, continuous models, and hybrid models. Discrete models, such as agent-based or Cellular Potts-based approaches, follow the fate of each single cell or each cohort of cells over time. Due to the computational costs associated with implementing these models, they cannot capture aspects of tissue mechanics effectively and they can only model subdomains of the whole tumour [14]. Continuous models describe cancerous tissues as domains composed of multiple phases interacting with each other. Finally, hybrid models incorporate different aspects of discrete and continuous models [15]. Tumour models range from macroscopic models that describe volumetric tumour growth to others that enable simulation of important molecular processes. In this case, a cell's proliferation and death rates are modulated by its genotype and phenotype, and by the therapeutics that reach the tumour cells. The modulation of cell proliferation and death rates by chemotherapeutic agents is best described in term of signalling pathways within a single cell, e.g., by intracellular models [16]. The effects of paracrine signalling, cell-to-cell physical interactions, and the local metabolic conditions (most importantly, oxygenation) are best described by multi-cellular models that represent the collective behaviour of a large cellular population [14]. Finally, the biomechanical interactions of the growing tumour with other organs, and the diffusion-reaction of metabolites are best represented at the whole-tumour scale. While in theory, it is possible to describe this entire process with a single mathematical model, in practice, there are limitations due to the resolution of the data used to parameterise the model and the computational power available to solve it numerically. Therefore, such a brute-force approach is impossible, unless the single-scale cancer model is extremely idealised [17]. Thus, most models of tumour growth comprise multiple component models, each describing the phenomenon at a specific space-time scale [18] [19] [20]. In this work, we shift our attention from multiscale models to continuum-based models; a detailed review of cancer models can be found here [21] [22]. Continuous models have the potential to absorb patient-specific data, such as those coming from anatomical magnetic resonance imaging, diffusion tensor imaging and perfusion imaging [23]. Also, as multiple treatment

protocols are made available, it is important to develop so-called Digital Twins, patient-specific computer models capable of predicting how a patient's tumour will respond to different treatments, thereby enabling the possibility of informing personalised treatment plans.

One major unresolved issue in developing such multiscale models concerns scale separation: how we split a multiscale model of a complex phenomenon into multiple models, each representing the phenomenon at a specific space-time scale. This critical decision is frequently neglected, and a scale separation is frequently adopted without justification, assuming a "natural" scale separation based on vague and qualitative anatomical concepts (cell, tissue, tumour). To the best of the authors' knowledge, the first paper to raise the issue of scale separation in this context is [24]. More recently, a theoretical framework was proposed, but for a much narrower problem [25]. One of the authors introduced the problem in [26], and proposed a general approach in [27]. This paper uses a similar theoretical approach to analyse the scale separation of a tumour growth model [28].

This study aims to explore the scale separation of a new multiscale tumour growth model being developed in the PRIMAGE project [29] to personalise the treatment of neuroblastoma patients, with the objectives of minimising the model complexity and respecting the experimental resolution and computational constraints that limit scale ranges.

MATERIALS AND METHODS

Scale separation

In the following, a scale is defined in terms of grain and extent. The grain is the largest value between the lower limit of spatial/temporal resolution allowed by the instrumentation, and the smallest/fastest feature of interest to be observed. Similarly, the extent is the smallest value between the upper limit of spatial/temporal resolution (i.e., the region of interest in a four-dimensional space) and the size of the largest/slowest feature of interest to be observed. The resolution is the smallest interval of a measured quantity that can still cause a change in the measurement result [26].

Generally speaking, the mechanistic description of tumour growth spans a dimensional extent that goes from the molecular scale (10-10 m) to the whole-tumour scale (10-1 m),

and temporally from fast chemical reactions (10-3 s) to the clinical follow-up (5 years, 108 s). Since no experimental method has enough resolution to provide this spatiotemporal grain over such a large spatiotemporal extent, and since in any case, no computer has enough computational power to solve such a model, tumour growth models are almost always (explicitly or implicitly) multiscale models or macroscopic continuum models.

In a way, even single-scale models are (implicitly) multiscale. Single-scale models typically describe only a portion of the extent with a grain larger than the smallest necessary grain. Everything beyond the extent considered is lumped into boundary conditions, and everything below the grain considered is lumped into constitutive equations. However, these lumping operations can be grossly inaccurate, and they hide some key elements of the process (all those above and below the scale of the model) that we might need to predict. The alternative is the use of explicitly multiscale models, which are orchestrations of single-scale models (component models) linked together by data transformation services (relation models) that transform the quantities at one scale to those at another scale (sometimes referred to as homogenization, when they transform from a small scale to a large one, and particularization, when they transform in the opposite direction).

When designing a multiscale model, a key decision concerns scale separation, e.g., the grain and extent that each component model represents. In much of the literature, this operation is defined in terms of abstract, qualitative concepts rooted in anatomy or histology (tumour scale, tissue scale, etc). However, space-time is a continuum, and the decision to partition it into separate scales must be made based on the model's purpose, the resolution of the instrumentation used to inform and validate the model, and the computational power available. The approach we propose to define scale separation, first described in [27], requires as the first step, the definition of a mathematical model that provides the infinite resolution idealisation of the multiscale model being developed.

Idealisation of tumour growth: macroscopic continuum model

Neuroblastoma tumours comprise a large variety of cells. We assume that a cell's type i in this case, is binary: cells originating from the neural crest (i = s) and those from radial glial cells (i = n). Following the theory of cancer stem cells [30], we will consider the first group cancer Schwann cells, and the second cancer Neuroblast cells.

The probability that a cell k in an untreated tumour changes its internal state γ_k to replication or death π_(γ_k), is a function of the cell's type (I_k), its differentiation level (α_k), and the local concentration of the chemical species of interest (Sj):

$$\pi_{\gamma_k}(k(X), t) = \pi_{\gamma_k}\big(I_k, \alpha_k, \tau_k, S_1, \dots, S_J, t\big). \qquad (1)$$

The probability that the cell proliferates or dies depends on the internal state of the cell and the chemical signals encoded by the concentration dynamics of specific chemical species Sj in the region of the cell. These chemical species (Sj) are supplied to the tumour volume and consumed by the tumour cells:

$$\dot{S}_j(X,t) = \sum_k^{N \in dV_X} \chi_k^j(I_k, \alpha_k, \gamma_k, \tau_k, t) + \sum_k^{N \in dV_X} \sigma_k^j(I_k, \alpha_k, \gamma_k, \tau_k, t), \quad (2)$$

where:

X is a generic point within the tumour,

t is the time,

$\dot{S}_j$ is the rate of change of chemical species j at point X of the tumour at time t,

χ_k^j is the rate of consumption of the chemical species j by cell k,

σ_k^j is the rate of supply of the chemical species j by cell k,

I_k is the type of cell k,

α_k is the level of differentiation of cell k, from fully undifferentiated stem cells (α = 0), to fully differentiated cells (α = 1),

γ_k is the internal state of cell k,

τ_k is the telomerase state of cell k, and

N is the number of cells inside the infinitesimal neighbourhood of point X (see definition below).

The difference between the proliferation rate of cells of type i and differentiation state α, f_p^(i,α), and the rate of cell death, f_d^(i,α), represents the rate of change of the number of cells of type i in the volume dVX:

$$r_i^{dV_X}(X,t) = f_p^{i,\alpha}(X,t) - f_d^{i,\alpha}(X,t) = \frac{dC_i^{dV_X}(X,t)}{dt}. \qquad (2)$$

The proliferation rate of cells of type i located within the infinitesimal volume dVX associated with point X at time t is:

$$r_i^{dV_X(X,t)} = \frac{dC_i^{dV_X}(X,S_1,\ldots,S_J,t)}{dt} \quad (4)$$

Ci represents the concentration of cells of type i, regardless of their differentiation level. Thus, the conservation of mass for the cells of type i can be written as:

$$\frac{\partial C_i^{dV_X}(X,t)}{\partial t} + \nabla \cdot \left(C_i^{dV_X}(X,t) \frac{\partial u(X,t)}{\partial t} \right) = r_i^{dV_X}, \quad (3)$$

where dVX is its infinitesimal neighbourhood, u is the displacement of the extracellular matrix caused by the growth of the tumour and by its deformation against the surrounding tissues and organs at that point and at that time.

The total volume of the tumour V at any point in time is due to the sum of the cellular volume and Extra-Cellular Matrix (ECM) volume. However, for a given level of cellularity, the ECM volume will change proportionally to the cellular volume. Since every cell has a similar volume, the cellular volume is proportional to the number of cells in the volume V, CV. Thus, we can write:

$$\frac{\partial V}{\partial t} = k^{i\alpha} \left(\frac{\partial C^V}{\partial t} \right) = k^{i\alpha} \left(\frac{\partial C_S^V}{\partial t} + \frac{\partial C_n^V}{\partial t} \right) \quad (4)$$

in which i represents the cell type and α the differentiation state.

If W is a topological space that represents the tumour volume, and X is a point in W, we will define dVX as an infinitesimal neighbourhood of X, which is any subset of W that includes an open set containing X and whose volume tends to zero. Thus, while continuous variables such as the concentration of a chemical species are associated with a generic point X, discrete variables like the number of cells are associated with the infinitesimal neighbourhood of X, dVX.

Until now, we were considering tumour growth in the absence of treatment. Once a tumour is diagnosed, the oncologist can usually choose from a small number of alternative options for treatment. In theory, each of those treatments should slow down, or even reverse the tumour's growth. In practice, this largely depends on the genetic makeup of the tumour. Considering this, the probability for cell k to change its internal state can be written as:

$$\pi^{*}_{\gamma_k}(k(X), T_l, t) = \pi_{\gamma_k}\left(I_k, \alpha_k, \tau_k, S_1, \dots, S_J, t\right) \cdot \pi^{treat}_{\gamma_k}(T_l), \tag{5}$$

where

π_(γ_k)^* is the cumulative probability of internal state change for cell k and Tl l = 1, L is the treatment type, in a scenario where multiple treatment options are available. Assembling all these equations, the mathematical model that describes the growth of the tumour defined above can be written as the equations below.

$$\begin{cases} \pi^{*}_{\gamma_k}(k(X), T_l, t) = \pi_{\gamma_k}\left(I_k, \alpha_k, \tau_k, S_1, \dots, S_J, t\right) \cdot \pi^{treat}_{\gamma_k}(T_l) \\ r_i^{dV_X}(X,t) = \dfrac{dC_i^{dV_x}\left(X, S_1, \dots, S_J, t\right)}{dt} \\ \dot{S}_j(X,t) = \sum_{k}^{N \in dV_X} \chi_k^j(I_k, \alpha_k, \gamma_k, \tau_k, t) + \sum_{k}^{N \in dV_X} \sigma_k^j(I_k, \alpha_k, \gamma_k, \tau_k, t) \\ r_i^{dV_X}(X,t) = f_p^{i,a}(X,t) - f_d^{i,a}(X,t) = \dfrac{dC_i^{dV_X}(X,t)}{dt} \\ \dfrac{\partial C_i^{dV_X}(X,t)}{\partial t} + \nabla \cdot \left(C_i^{dV_X}(X,t)\dfrac{\partial u(X,t)}{\partial t}\right) = r_i^{dV_X} \\ \dfrac{\partial V}{\partial t} = k^{ia}\left(\dfrac{\partial C^V}{\partial t}\right) = k^{ia}\left(\dfrac{\partial C_s^V}{\partial t} + \dfrac{\partial c_n^V}{\partial t}\right) \end{cases} \tag{6}$$

A multiscale framework for modelling growth of solid tumours

In our multiscale framework, we divide the spatial domain of the tumour into three levels using a hybrid numerical approach (see Fig. 1). On the one hand, using patient-specific images of the geometry and the corresponding DTI-MRI biomarkers, we propose to develop a patient-specific Finite Element Model (FEM) of the whole tumour. From the extent of vascularisation, the spatiotemporal distribution of nutrients and oxygen in the tumour are computed. Through particularisation this information is used at the tissue scale to evaluate how cells behave according to different levels of oxygen and nutrients, regulating cell proliferation, differentiation, hypoxia, and matrix formation. For this purpose, we propose to use an agent-based model (ABM) to describe these behaviours, taking into consideration cell-cell and cell-matrix interactions. Each cell agent is evaluated individually to update cell state reflecting behaviours such as proliferation and apoptosis/necrosis according to the current cell state (including genetic/molecular factors) and the current condition of the local microenvironment (e.g., concentration of oxygen, chemotherapeutics drugs, cell crowding). Cell proliferation/death and matrix formation both influence emergent tumour growth. The growth of the reference volume explicitly simulated using this agent-based approach is incompatible with the other reference volumes in the model, inducing the mechanical

residual strains/stresses characteristic of solid tumours [31]. By means of an iterative process, we guarantee the compatibility between different regions of the tumour. Consequently, the new spatial configuration of the matrix and the cell population will be computed by means of homogenization, which links the ABM to the macroscopic scale.

Example of application: neuroblastoma

Neuroblastoma (NB) is the most common extra-cranial paediatric solid tumour, accounting for 7% of childhood malignancies. Contrary to most other paediatric malignancies, high-risk NB is fatal in almost half of the patients diagnosed. NB arises from the primordial neural crest cells that form the sympathetic nervous system and is usually found around the adrenal glands [32]. Approximately, 60-70% of the cases are metastatic at presentation. NB is a strongly heterogeneous cancer, with strikingly different clinical outcomes. These characteristics are shared with many other cancer types, and hence NB can be considered a paradigm of the general cancer disease and an excellent context in which to validate novel developments aiming to be applicable in a large variety of cancers. The International Neuroblastoma Pathology Classification (INPC) classifies NB patients into those with favourable or unfavourable post-surgical histology. Depending on the Schwannian stroma development, tumours can be classified as Schwannian stroma–rich or poor. Three finer diagnostic categories of the former category are mature ganglioneuroma, intermixed ganglioneuroblastoma, and nodular ganglioneuroblastoma. Three categories of Schwannian stroma–poor neuroblastoma are: differentiated, poorly differentiated, and undifferentiated. As tumour aggressiveness is linked to the INPC histological features, in clinical practice, treatments for cases with different neuroblastic grades are quite different.

Initial dimensional analysis

Neuroblastomas can be as large as 800 cc (around 100 mm in diameter, assuming a spherical shape), or so small as to be barely segmented in an abdominal MRI (1.0 cc, 10 mm in diameter). The effect of chemotherapy on neuroblastoma cells can be modelled at the single-cell scale, so the extent here is around 10 mm. The grain should be that of the therapeutic molecule (assuming a molecular weight of 500 Da, the molecule size is around 5-10 nm). Therefore, the infinite resolution model would need to model a spatial extent up to 10-1 m with a grain of 10-8 m.

The definition of the temporal extent is more complex. Neuroblastoma patients typically receive up to three chemotherapy cycles, every eight weeks, so if the model is used to simulate the whole duration of the therapy, the temporal extent will be 24 weeks (107 s). The temporal grain is defined by the time required by specific biochemical reactions; while it is very difficult to be specific, these are usually of the order of 10-2 s.
So, the hypothetical infinite resolution model would span nine orders of magnitude both in time and space. This is clearly intractable, so a multiscale model is necessary.

Limits to scale separation

The upper and lower limits in space and time are dictated by the problem itself, as defined in the infinite resolution model. Thus, the spatial extent of the tumour model is set by the size of the solid tumour. The spatial grain of the tumour model is limited by the resolution of the medical imaging instrumentation that is used to define the 3D geometry of the tumour; assuming the modality is an MRI, the typical image resolution is 1–2 mm. The grain is also limited by the number of degrees of freedom (NDOF) that the finite element method can reasonably solve. Assuming the NDOF's upper limit is 106, the average element size is around 1.5 mm.
The temporal extent of the tumour model is the duration of the chemotherapy: up to 24 weeks. The experimental limitation on the grain is the minimum distance between two successive imaging controls; if we assume a CT scan is performed before each new chemotherapy cycle, a scan will be performed once every 1-3 months. The evolution of the tumour growth, as predicted by the model, show be provided, to be clinically relevant, with a granularity of at least two weeks.
The extent of the tissue model is conveniently set at the same size as the grain of the tumour model (Table I). Note that here we refer to a model of behaviour and interactions between the microenvironment of the stroma and cells, or intercellular interactions, including cells that are native (e.g., Schwann cells) and non-native (i.e., potentially cancerous). This way we can avoid the need for a relation model here. However, a relation model remains necessary to interpolate between initial conditions. A tumour model with 300,000 elements requires the tissue model to run 300,000 times at each time step of the tumour model.

Within the context of the PRIMAGE project, the tissue model is an ABM which needs to be implemented on a GPU node, and the available HPC system allows the simultaneous use of 100 nodes with such configurations. Thus, we consider, for simplification, that we can afford to run 100 tissue models for each tumour time step.

The relation model should partition the range of initial conditions into an appropriate number of bins. Similarly, we need a relation model that, when given the 100 predictions from the tissue model, can interpolate them to the 300,000 values required by the tumour model.

TABLE I
Space-time grain and extent for the presented multiscale model.

	Space		***Time***	
Nickname	*Extent*	*Grain*	*Extent*	*Grain*
Tumour	Upper limit 10^-1 m	CT resolution 10^-3 m	Upper limit 10^7 s	imaging controls 10^5 s
		Solvable NDOF 10^-3 m		Time steps 10^5 s
Tissue	From Tumour 10^-3m	cell size 10^-5 m	From Tumour 10^5 s	Cultures controls 10^3 s
		Solvable agents 5*10^-5 m		Time steps 10^4 s
Cell	From Tissue 10^-5 m	Lower limit 10^-8 m	From Tissue 10^5 s	Lower limit 10^-2 s

The spatial extent of the tissue model is equal to the spatial grain of the tumour model. The grain of the tissue model is limited experimentally by the average cell size, and computationally by the number of autonomous agents the model can handle simultaneously. In a cube measuring 2 mm in each dimension, there are 8 million cells with a diameter of 10 microns, but assuming that cells occupy only 80% of the tissue volume in neuroblastoma, we need 6.400,000 agents.

The temporal extent of the tissue model is equal to the temporal grain of the tumour model. The temporal grain of the tissue model is limited computationally by the maximum time step that ensures an acceptable discretisation error for the tissue model.

The spatial and temporal extents of the tissue model are respectively equal to the spatial and temporal grain of the tumour model. The probabilistic and phenomenological nature of the cell model does not require mechanistic modelling of molecules; thus, this model has no grain, strictly speaking. The cell model is not coupled to the tissue model. It is run once,

separately, taking as its inputs the genetic markers of the tumour and the list of chemotherapeutic options, and returning the probability with which each drug will amplify or suppress each cellular pathway. In particular, in the tissue model, the rates of cellular events such as replication or cell death will be altered according to the probabilities that the cell model predicts for the relevant pathways.

Based on this analysis, the presented neuroblastoma multiscale model can be summarised with a scale separation map (Fig. 1).

The main variables that are exchanged between the scales are illustrated by Fig. 1. The concentrations of chemical species, S ̇_j (X,t), are sampled and interpolated between the tissue and tumour scales. The volume (V) is sampled from Tumour to tissue and the variation of volume over time (∂V/∂t) is interpolated back from tissue to Tumour. The Cell scale provides the tissue scale with the probability of an agent changing its internal state depending on the therapeutic option chosen (π_(γ_k)^*).

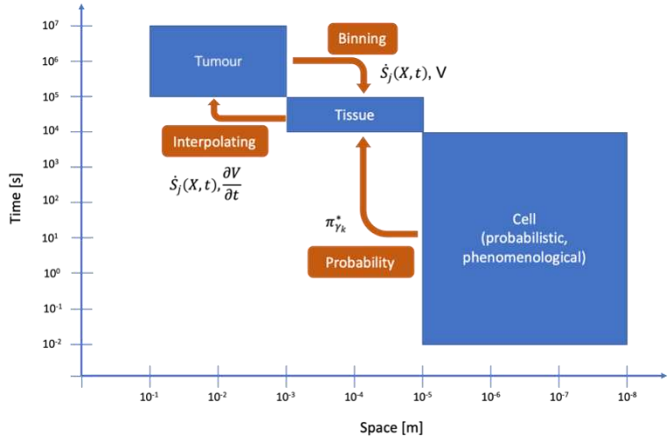

Fig. 1. Scale separation map for multiscale tumour growth model.

DISCUSSION

The aim of this study was to find the scale separation of a new multiscale tumour growth model that minimises the modelling complexity, while respecting the experimental resolution and computational constraints that limit the scale ranges. To this end, we used an approach first proposed in [27], which tackles the problem by considering a multiscale model as an engineering construct, optimised on the basis of the experimental and computational limitations imposed by the available methods, rather than on the basis of abstract mathematical considerations.

To evaluate the difference in expected accuracy between the approach presented herein for the scale separation and the idealised model, we would have to solve the latter at least once, which is currently impractical. It is possible, however, to calculate the error introduced by the particularisation step, by solving at least once the whole multiscale model without using any binning strategy for particularisation, assuming that one instance of the ABM will be run for each Finite Element in the Tumour scale model and then comparing the outcome to a simulation that includes fewer ABM instances, using a binning strategy for interpolation of the results back to the Tumour scale model. The details of the quantification of the error resulting from the particularisation step fall outside of the scope of this paper and are described in [34]. It is reasonable to expect that this step is the most critical in terms of predictive accuracy. For a large volume, the reduction of hundreds of thousands of finite elements into only a hundred ABMs is surely a major simplification; while more sophisticated sampling and interpolation techniques can reduce the impact on accuracy, the particularisation step becomes, for large tumours, so brutal that large predictive errors are unavoidable. In this sense, the race for exascale computing is helpful: the pre-exascale Summit supercomputer at Oak Ridge National Laboratory (USA) has 27,648 NVIDIA Tesla GPUs; by contrast, in Europe, the pre-exascale Leonardo supercomputer, to be installed at CINECA (Italy) before the end of 2021, will offer 13,824 NVIDIA A100 GPUs; these new GPUs are expected to be at least two to three times faster than the Tesla GPUs.
The main limitation of the multiscale cancer model we described is that, at the moment, it lacks a single-cell component model that can use the genomic data obtained from a tumour biopsy to predict the replication and apoptotic rates for the various cell types, as well as the effects of different chemotherapeutic drugs on these rates. Another limitation is that we are not considering metastasis which is the spread of cancer cells to other tissues and organs [33]. However, the scale separation approach, which is the main focus of this paper, is effective for designing multiscale models of solid tumour growth.
Every paper that describes a multiscale model should provide a justification for its scale separation based on the resolution of the experimental methods available to inform the model, and the computational power available for its solution.

ACKNOWLEDGEMENTS

This study was funded by PRIMAGE (PRedictive In-silico Multiscale Analytics to support cancer personalized diaGnosis and prognosis, empowered by imaging biomarkers), a Horizon 2020|RIA project (Topic SC1-DTH-07-2018), grant agreement no: 826494. JMGA was also supported by the Spanish Ministry of Science, Innovation and Universities (RTI2018-094494-BC21) and the Government of Aragon in the form of grants awarded to SHR (Grant No. 2019-23).

Author's contributions

MV proposed the scale separation project. MV, BMQ, JMGA and SHR contributed to the design of the mathematical model. All authors contributed to writing and approved the final manuscript.

REFERENCES

[1] H. Sung et al., 'Global cancer statistics 2020: GLOBOCAN estimates of incidence and mortality worldwide for 36 cancers in 185 countries', CA: A Cancer Journal for Clinicians, vol. n/a, no. n/a, doi: https://doi.org/10.3322/caac.21660.

[2] J. L. Connolly, S. J. Schnitt, H. H. Wang, J. A. Longtine, A. Dvorak, and H. F. Dvorak, 'Tumor Structure and Tumor Stroma Generation', Holland-Frei Cancer Medicine. 6th edition, 2003, Accessed: Jun. 13, 2021. [Online]. Available: https://www.ncbi.nlm.nih.gov/books/NBK13447/

[3] Q. Liu, Q. Luo, Y. Ju, and G. Song, 'Role of the mechanical microenvironment in cancer development and progression', Cancer Biol Med, vol. 17, no. 2, pp. 282–292, May 2020, doi: 10.20892/j.issn.2095-3941.2019.0437.

[4] J. Plou, Y. Juste-Lanas, V. Olivares, C. del Amo, C. Borau, and J. M. García-Aznar, 'From individual to collective 3D cancer dissemination: roles of collagen concentration and TGF-β', Sci Rep, vol. 8, no. 1, Art. no. 1, Aug. 2018, doi: 10.1038/s41598-018-30683-4.

[5] 'Extracellular matrix density regulates the formation of tumour spheroids through cell migration'. https://journals.plos.org/ploscompbiol/article?id=10.1371/journal.pcbi.1008764 (accessed Jun. 04, 2021).

[6] J. Escribano et al., ‘Balance of mechanical forces drives endothelial gap formation and may facilitate cancer and immune-cell extravasation’, PLOS Computational Biology, vol. 15, no. 5, p. e1006395, May 2019, doi: 10.1371/journal.pcbi.1006395.

[7] D. Hanahan and R. A. Weinberg, ‘Hallmarks of Cancer: The Next Generation’, Cell, vol. 144, no. 5, pp. 646–674, Mar. 2011, doi: 10.1016/j.cell.2011.02.013.

[8] T. Otto and P. Sicinski, ‘Cell cycle proteins as promising targets in cancer therapy’, Nat Rev Cancer, vol. 17, no. 2, pp. 93–115, Jan. 2017, doi: 10.1038/nrc.2016.138.

[9] F. Mantovani, L. Collavin, and G. Del Sal, ‘Mutant p53 as a guardian of the cancer cell’, Cell Death Differ, vol. 26, no. 2, pp. 199–212, Feb. 2019, doi: 10.1038/s41418-018-0246-9.

[10] S. Ackermann et al., ‘A mechanistic classification of clinical phenotypes in neuroblastoma’, Science, vol. 362, no. 6419, pp. 1165–1170, Dec. 2018, doi: 10.1126/science.aat6768.

[11] X. Jiang et al., ‘The role of microenvironment in tumor angiogenesis’, Journal of Experimental & Clinical Cancer Research, vol. 39, no. 1, p. 204, Sep. 2020, doi: 10.1186/s13046-020-01709-5.

[12] E. R. Pastor and S. A. Mousa, ‘Current management of neuroblastoma and future direction’, Critical Reviews in Oncology/Hematology, vol. 138, pp. 38–43, Jun. 2019, doi: 10.1016/j.critrevonc.2019.03.013.

[13] P. M. Altrock, L. L. Liu, and F. Michor, ‘The mathematics of cancer: integrating quantitative models’, Nat Rev Cancer, vol. 15, no. 12, Art. no. 12, Dec. 2015, doi: 10.1038/nrc4029.

[14] J. Metzcar, Y. Wang, R. Heiland, and P. Macklin, ‘A Review of Cell-Based Computational Modeling in Cancer Biology’, JCO Clinical Cancer Informatics, no. 3, pp. 1–13, Feb. 2019, doi: 10.1200/CCI.18.00069.

[15] K. A. Rejniak and A. R. A. Anderson, ‘Hybrid models of tumor growth’, Wiley Interdiscip Rev Syst Biol Med, vol. 3, no. 1, pp. 115–125, Feb. 2011, doi: 10.1002/wsbm.102.

[16] E. Kozłowska, R. Suwiński, M. Giglok, A. Świerniak, and M. Kimmel, ‘Mathematical model predicts response to chemotherapy in advanced non-resectable non-small cell lung cancer patients treated with platinum-based doublet’, PLOS Computational Biology, vol. 16, no. 10, p. e1008234, Oct. 2020, doi: 10.1371/journal.pcbi.1008234.

[17] S. Bekisz and L. Geris, ‘Cancer modeling: From mechanistic to data-driven approaches, and from fundamental insights to clinical applications’, Journal of Computational Science, vol. 46, p. 101198, Oct. 2020, doi: 10.1016/j.jocs.2020.101198.

[18] V. Vavourakis, P. A. Wijeratne, R. Shipley, M. Loizidou, T. Stylianopoulos, and D. J. Hawkes, ‘A Validated Multiscale In-Silico Model for Mechano-sensitive Tumour Angiogenesis and Growth’, PLoS Comput Biol, vol. 13, no. 1, p. e1005259, Jan. 2017, doi: 10.1371/journal.pcbi.1005259.

[19] L. Peng, D. Trucu, P. Lin, A. Thompson, and M. A. J. Chaplain, ‘A Multiscale Mathematical Model of Tumour Invasive Growth’, Bull Math Biol, vol. 79, no. 3, pp. 389–429, Mar. 2017, doi: 10.1007/s11538-016-0237-2.

[20] F. Pourhasanzade and S. H. Sabzpoushan, ‘A New Mathematical Model for Controlling Tumor Growth Based on Microenvironment Acidity and Oxygen Concentration’, Biomed Res Int, vol. 2021, p. 8886050, 2021, doi: 10.1155/2021/8886050.

[21] T. S. Deisboeck, Z. Wang, P. Macklin, and V. Cristini, ‘Multiscale Cancer Modeling’, Annu. Rev. Biomed. Eng., vol. 13, no. 1, pp. 127–155, Jul. 2011, doi: 10.1146/annurev-bioeng-071910-124729.

[22] J. S. Lowengrub et al., ‘Nonlinear modelling of cancer: bridging the gap between cells and tumours’, Nonlinearity, vol. 23, no. 1, p. R1, Dec. 2009, doi: 10.1088/0951-7715/23/1/R01.

[23] S. Angeli, K. E. Emblem, P. Due-Tonnessen, and T. Stylianopoulos, ‘Towards patient-specific modeling of brain tumor growth and formation of secondary nodes guided by DTI-MRI’, Neuroimage Clin, vol. 20, pp. 664–673, 2018, doi: 10.1016/j.nicl.2018.08.032.

[24] D. J. W. Evans et al., ‘The application of multiscale modelling to the process of development and prevention of stenosis in a stented coronary artery’, Philos Trans A Math Phys Eng Sci, vol. 366, no. 1879, pp. 3343–3360, Sep. 2008, doi: 10.1098/rsta.2008.0081.

[25] S. Chakraborty, S. Raju, and R. K. Pal, ‘A multiscale three-zone reactive mixing model for engineering a scale separation in enzymatic hydrolysis of cellulose’, Bioresour Technol, vol. 173, pp. 140–147, Dec. 2014, doi: 10.1016/j.biortech.2014.09.088.

[26] P. Bhattacharya and M. Viceconti, ‘Multiscale modeling methods in biomechanics’, WIREs Systems Biology and Medicine, vol. 9, no. 3, p. e1375, 2017, doi: 10.1002/wsbm.1375.

[27] P. Bhattacharya, Q. Li, D. Lacroix, V. Kadirkamanathan, and M. Viceconti, 'A systematic approach to the scale separation problem in the development of multiscale models', PLoS One, vol. 16, no. 5, p. e0251297, 2021, doi: 10.1371/journal.pone.0251297.

[28] K.-A. Norton, C. Gong, S. Jamalian, and A. S. Popel, 'Multiscale Agent-Based and Hybrid Modeling of the Tumor Immune Microenvironment', Processes (Basel), vol. 7, no. 1, Jan. 2019, doi: 10.3390/pr7010037.

[29] L. Martí-Bonmatí et al., 'PRIMAGE project: predictive in silico multiscale analytics to support childhood cancer personalised evaluation empowered by imaging biomarkers', European Radiology Experimental, vol. 4, no. 1, p. 22, Apr. 2020, doi: 10.1186/s41747-020-00150-9.

[30] M. F. Clarke et al., 'Cancer stem cells--perspectives on current status and future directions: AACR Workshop on cancer stem cells', Cancer Res, vol. 66, no. 19, pp. 9339–9344, Oct. 2006, doi: 10.1158/0008-5472.CAN-06-3126.

[31] T. Stylianopoulos, 'The Solid Mechanics of Cancer and Strategies for Improved Therapy', Journal of Biomechanical Engineering, vol. 139, no. 2, p. 021004, Feb. 2017, doi: 10.1115/1.4034991.

[32] J. M. Maris and K. K. Matthay, 'Molecular Biology of Neuroblastoma', JCO, vol. 17, no. 7, pp. 2264–2264, Jul. 1999, doi: 10.1200/JCO.1999.17.7.2264.

[33] T. A. Martin, L. Ye, A. J. Sanders, J. Lane, and W. G. Jiang, Cancer Invasion and Metastasis: Molecular and Cellular Perspective. Landes Bioscience, 2013. Accessed: Apr. 22, 2021. [Online]. Available: https://www.ncbi.nlm.nih.gov/books/NBK164700/

[34] [1]

Vinicius Varella, Bárbara de Melo Quintela, Marek Kasztelnik, e Marco Viceconti, "Effect of Particularisation size on the Accuracy and Efficiency of a Multiscale Tumours' Growth Model", International Journal for Numerical Methods in Biomedical Engineering, (submitted).